Journal of Inflammation Research Dovepress

Open Access Full Text Article ORIGINAL RESEARCH

Higher Expression of Ku80 and Ku70 Indicates Hotter Tumor Immune Microenvironment in Hepatocellular Carcinoma and Better CTL-Centered Immunotherapy

Lukun Yang[1,2,*], Ling Li[3,*], Peiping Li[1,*], Jiafan Chen[1], Chaonong Cai[1], Yingbin Jia[1], Jian Li[1], Baojia Zou[1]

[1]Department of Hepatobiliary Surgery, The Fifth Affiliated Hospital of Sun Yat-Sen University, Zhuhai, Guangdong Province, People's Republic of China; [2]Department of Anesthesiology, The Fifth Affiliated Hospital of Sun Yat-sen University, Zhuhai, Guangdong Province, People's Republic of China; [3]Department of Pharmacy, The Fifth Affiliated Hospital, Sun Yat-Sen University, Zhuhai, Guangdong, People's Republic of China

*These authors contributed equally to this work

Correspondence: Baojia Zou; Jian Li, Department of Hepatobiliary Surgery, The Fifth Affiliated Hospital of Sun Yat-sen University, 52 Mei Hua East Road, Zhuhai, 519000, People's Republic of China, Tel +86-756-252-8781, Fax +86-756-252-8166, Email zoubj6@mail.sysu.edu.cn; lijian5@mail.sysu.edu.cn

Purpose: Both Ku80 and Ku70 are promising drug targets for hepatocellular carcinoma (HCC) and crucial for immune regulation. However, their correlation with HCC immune signatures has not yet been investigated. Therefore, we aimed to investigate the relationship between Ku80, Ku70, and immune signatures in HCC and validate their significance in cytotoxic lymphocyte (CTL) immunotherapy.

Patients and Methods: Analyses of Ku70, Ku80, and immune signatures in public datasets was performed using R software, an online Kaplan-Meier plotter, g:Profiler, GeneTrail, and Metascape. Uniform manifold approximation and projection, correlation chord diagrams, Pearson's correlation tests, and Spearman correlation tests were used to describe various correlation levels. HCC mRNA sequencing data (n=373 tumor samples and n=50 para-tumor samples) were drawn from The Cancer Genome Atlas (TCGA) public database. Immunofluorescent staining was used to validate Ku70/Ku80 and $CD8^+$CTL expression in 120 HCC patients from our center. Survival analysis was performed using the Kaplan-Meier survival analysis with the Log rank test and was adopted to analyze immunotherapy outcomes correlated with Ku70/Ku80 expression in various solid tumors. Multivariate analysis of HCC patient data from our center was performed using a Cox proportional hazards model.

Results: Increased Ku70/Ku80 expression positively correlated with more enriched immune microenvironment signatures, indicating increased immune infiltration in HCC. Upregulation of Ku70/Ku80 indicated better anti-PD1 and anti-PDL1 treatment outcomes in various solid tumors. Higher Ku70/Ku80 expression with lower $CD8^+$CTL signatures indicated worse survival outcomes, whereas lower Ku70/Ku80 expression with higher $CD8^+$CTL signatures indicated the best prognosis.

Conclusion: Higher Ku70/Ku80 expression indicated an immune-hot infiltration signature in HCC. Patients with increased Ku70/Ku80 expression and high $CD8^+$CTL signatures may potentially benefit from CTL-centered immunotherapies.

Keywords: hepatocellular carcinoma, XRCC6/Ku70, XRCC5/Ku80, CTL-centered immunotherapy, tumor immune microenvironment

Background

Hepatocellular carcinoma (HCC) is one of the most fatal malignancies worldwide. Increasing evidence has demonstrated the efficacy of immunotherapy in the treatment of patients with HCC, which relies largely on the immune status of tumors. Therefore, immunotherapy can only reach an objective response rate (ORR) of 30% or less in real world.[1,2] Many studies have been designed to understand and evaluate the tumor immune microenvironment, in the hope of

Received: 13 September 2024
Accepted: 12 November 2024
Published: 22 November 2024

finding a guide to HCC immunotherapy under different clinical scenarios.[3–5] However, much remains unknown about the HCC immune microenvironment. Understanding the HCC immune microenvironment is an essential step in the design and development of more potent immune-boosting agents.

Ku80 (coded by the gene *XRCC5*, X-ray repair cross complementing 5) and Ku70 (coded by the gene *XRCC6*, X-ray repair cross complementing 6) are important immune modulation factors in normal physiological conditions. They form the vital heterodimers in non-homologous end-joining (NHEJ) pathways and are crucial for repairing the DNA breaks in immune cells.[6–8] DNA breaks are more evident within the cancerous microenvironment, which suggests that the two Ku proteins are promising drug targets for the development of immune regulating agents in solid tumors.[9,10] Thus, both Ku proteins have long been considered important therapeutic targets in cancer.[11] Indirect activation of the NHEJ regulators can lead to increased anti-tumor $CD8^+$ cytotoxic lymphocytes (CTLs) via the recruitment of Ku proteins.[11] However, agents directly targeting the Ku proteins are still lacking due to the unknown relationship between Ku proteins and the tumor immune microenvironment.

Many immune cell types reside within the complicated tumor microenvironment. Myeloid cells, including neutrophils and macrophages, play bifunctional roles in cancer, whereas lymphocytes are key players in anti-cancer immunotherapies. $CD8^+$ CTL have been the most clinically relevant immune cells in current immunotherapies.[12] $CD4^+$ lymphocytes are traditionally regulatory lymphocytes, but also execute direct anti-tumor effect independent of CTL.[13] Additionally, natural killer cells (NKCs) are another anti-tumor cells.[14] Meanwhile, the presence of $CD4^+$ $CD25^+$ Foxp3 regulatory T cells (Tregs) contributes to a major cause of the immunosuppression in HCC.[15] Tregs interact with and regulate a wide spectrum of immune cells and are known targets of immunotherapies.[15] Both Ku proteins show vital regulatory effects on multiple immune cells in various conditions but their effects remain largely unknown in cancer.[16–21] For example, as mentioned above, Ku70 plays a role in the recruitment of the anti-tumor $CD8^+$CTL to cancer tissues.[11] However, the understanding of these immune cells and Ku proteins remains largely underexplored in HCC. Therefore, we hypothesized that Ku proteins could be closely associated with various intricate immune cells in HCC tumor microenvironment.

In the study, we aimed to investigate the potential relationship between Ku70, Ku80 and immune microenvironment signatures. We also validated the prognostic significance of Ku70 and Ku80 in CTL-centered immunotherapy. To confirm their prognostic roles in HCC, we performed a combined survival analysis of Ku80, Ku70 and $CD8^+$CTL in patients at our center. Thus, our data on the value of Ku80 and Ku70 in HCC immunotherapy will provide a basis for future studies.

Material and Methods

Analysis of the Interaction Between Ku70, Ku80, and the Immune Microenvironment Using Public Datasets

HCC mRNA sequencing data was drawn from The Cancer Genome Atlas (TCGA) database, and general characteristics of the patient data were described in our previous study (373 hCC tissues).[22] The etiology of most patients in the database included hepatitis, alcohol, cirrhosis and other risk factors. In brief, all data were downloaded from the National Cancer Institute GDC data portal, USA (https://portal.gdc.cancer.gov/). *R* software was used to analyze the sequencing data, which was downloaded from (https://cran.r-project.org/index.html). Morpheus (https://software.broadinstitute.org/morpheus) was used for optimized heatmap plotting. Gene ontology and gene set enrichment analyses was performed on https://biit.cs.ut.ee/gprofiler/gost,[23] and Genet rail (Enrichment analysis, Epigenetic analysis, Single cell analysis, Time series analysis) http://139.186.136.72:3838/Enrichtool2.3/,[24] and Metas cape http://metascape.org/gp/#/main/step1.[25]

Collected HCC Patient Samples for in vivo Validation of Ku80, Ku70, and CTL Signatures and Their Clinical Implications

Post-surgical patient samples (n=120) from our center were retrospectively analyzed. Immune fluorescence was used to examine the co-localization of Ku70/Ku80 and CD8 staining, as previously described.[26] In brief, the 4-μm thick slices were de-paraffinized and rehydrated via gradient alcohol concentrations. Tissues were subsequently blocked with the 5% BSA before exposure to primary antibodies. Primary antibodies were incubated at 4°C overnight. Tissues were then washed with PBS and incubated with fluorescence-conjugated secondary antibodies at room temperature for 60 minutes.

Finally, 2-(4-Amidinophenyl)-6-indolecarbamidine dihydrochloride (DAPI, BOSTER Biological Technology) was used for nucleus staining. The fluorescence microscope, ZEISS N-ACHROPLAN microscope (ZEISS, Germany) was used for analysis and photography. After immunofluorescence staining, Ku70/Ku80 expression was analyzed according to previously described methods.[26,27] All experimental protocols involving human samples, including analysis of data from publicly available data, were reviewed and approved by the Research Ethics Committee of the Fifth Affiliated Hospital of Sun Yat-sen University (reference number 2019-L-120-1).

Statistical Analysis

GraphPad Prism (version 9.0) and SPSS (version 29.0.1.0) software were used for the statistical analyses. Survival analysis was performed using the Kaplan–Meier survival analysis with Log rank test. An online Kaplan-Meier plotter was also used (http://kmplot.com/analysis/; http://www.oncolnc.org) to generate graphs. Survival outcomes for patients receiving immunotherapies based on the Ku70 and Ku80 expression status were also evaluated using the Kaplan-Meier plotter, which also hosts detailed data on several immunotherapies for various solid tumors.

A Student's *t* test was performed to compare two groups. One-way analysis of variance (ANOVA) was used to compare more than two groups. For correlation analyses, both Pearson's correlation tests and Spearman correlation tests were performed according to the different type of data. Pearson's or Spearman correlation coefficient, r, was used to describe the level of correlation between the analyzed factors. Uniform Manifold Approximation and Projection (UMAP) and correlation chord diagrams were analyzed and plotted via *R* software, to demonstrate the correlation between Ku70, Ku80 and various immune markers in the public datasets. Univariate analysis of the data of HCC patients from our center was performed by Kaplan-Meier survival analysis with a Log rank test. Multivariate analysis of the data of HCC patients from our center was performed by Cox proportional hazards models. Statistical significance was set at p-value <0.05. Not significance was abbreviated as N.S. The number of sample sizes is described in each figure.

Results

Expression of Ku80 and Ku70 Was Correlated with Different Intra-Tumoral Immune Signatures

The expression of Ku70 was significantly higher in tumor than in para-tumor expression (p <0.0001; Figure 1A). Higher intra-tumoral expression of Ku70 indicated poor prognosis in patients with HCC (hazard ratio [HR]=1.63, log-rank p=0.0003; Figure 1B). Likewise, the expression of Ku80 was significantly higher in tumors than in para-tumors (p = 0.0028; Figure 1C). Higher intra-tumoral expression of Ku80 also indicated a poor prognosis in HCC (HR=1.74, Log rank test p=0.0018, Figure 1D).

Generally, higher Ku70 and Ku80 expression levels correlated with different intra-tumoral immune signatures in HCC. Four different immune signatures were identified in HCC patients according to the expression levels of Ku proteins alone (Figure 1E), combined the Ku proteins with the common immune cell markers (Ku/immune 1, Figure 1E), combined with the common myeloid cell markers (Ku/immune 2, Figure 1E) and combined with the lymphocyte markers (Ku/immune 3, Figure 1E).

To investigate if the expression of Ku70 and Ku80 was indicative of the efficacy of current immunotherapies, the clinical outcomes of patients with T-cell centered immunotherapy were investigated with respect to the differential expression of tumoral Ku80 and Ku70. Since the sample size of HCC was small (n=22), we examined the pan-cancer immunotherapy data for the analysis of Ku70 and Ku80 across several solid tumors (including HCC, lung cancer, bladder cancer, glioblastoma, melanoma, etc). In the anti-PD1 therapy, high expression of both Ku80 and Ku70 was positively correlated with better treatment outcomes (Ku70, HR=0.66, log-rank p=0.0099; Ku80, HR=0.62, log-rank p=0.00087, Figure 1F). In anti-PDL1 therapy, high expression of both Ku80 and Ku70 was also positively correlated with better treatment outcomes (Ku70, HR=0.75, log-rank p=0.043; Ku80, HR = 0.8, log-rank p=0.099, Figure 1G). In sub-group analysis of patients with Pembrolizumab therapy, high expression of Ku70 and Ku80 correlated with better treatment outcomes and patient prognosis (Ku70, HR = 0.53, log-rank p=0.0025; Ku80, HR=0.49, log-rank p=0.00013, Figure 1H). However, the expression of Ku70 and Ku80 correlated with drastically different outcomes in anti-CTLA4 therapy (Figure 1I).

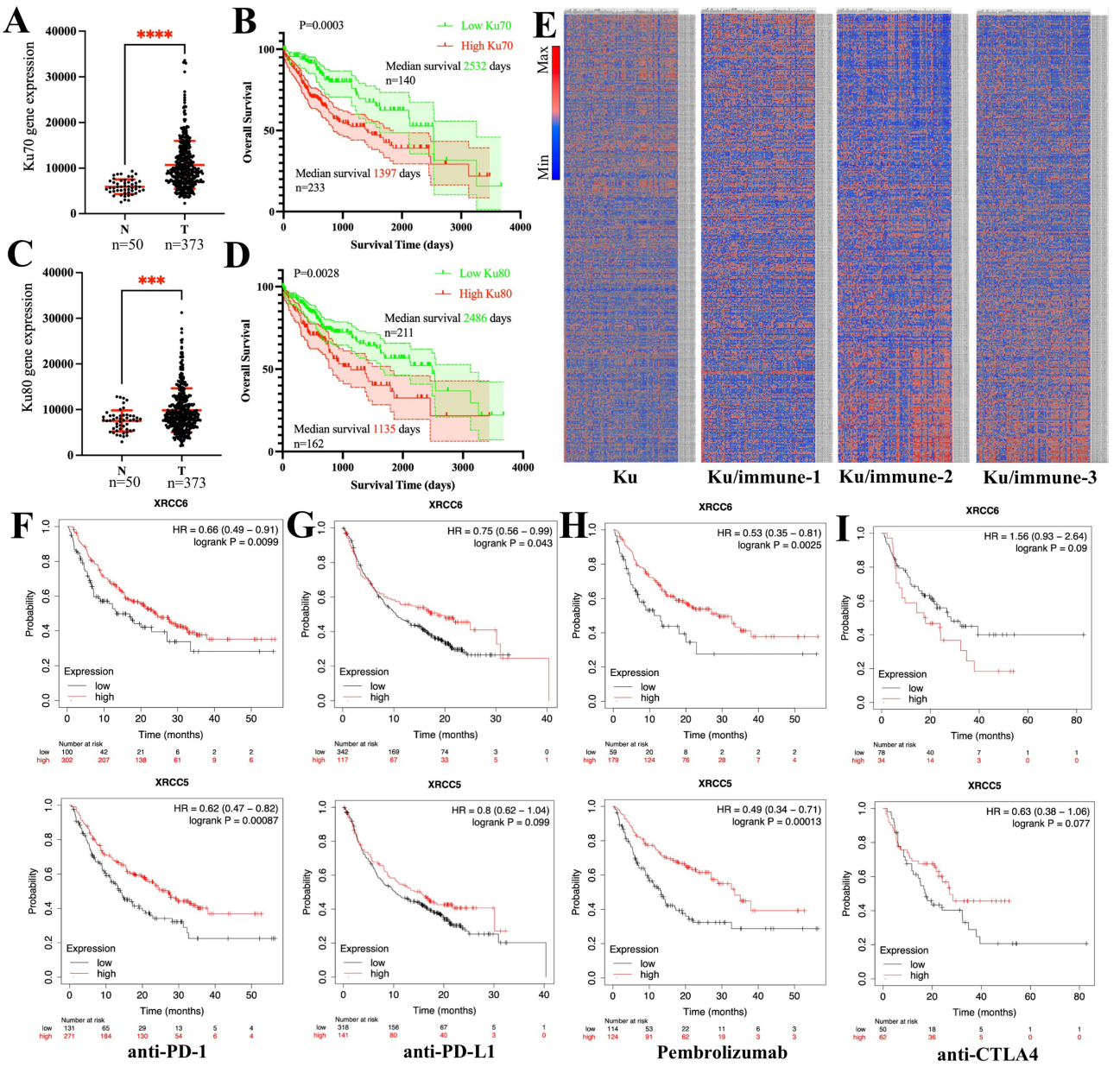

Figure 1 High expression of Ku70 and Ku80 indicated specific immune signatures and poor survival in HCC patients. (**A**). expression of Ku70 between para-tumor N and tumor T tissues. (**B**). overall survival of HCC patients with low Ku70 (green line) and high Ku70 (red line) expression (Log-rank p=0.0003). (**C**). expression of Ku80 between para-tumor N and tumor T tissues. (**D**). overall survival of HCC patients with low Ku80 (green line) and high Ku80 (red line) expression (Log-rank p=0.0028). (**E**). Heatmap revealed differential immune signatures regarding the expression of Ku70 and Ku80. Heatmap according to expression of Ku70/Ku80 alone (Ku), Ku70/Ku80 combined with the common immune cell markers (Ku/immune 1), Ku70/Ku80 combined with the common myeloid cell markers (Ku/immune 2) and combined with the lymphocyte markers (Ku/immune 3). Scale bar indicated high expression (red/max) to low expression (blue/minimum). (**F**). overall survival of patients receiving anti-PD1 therapy with low Ku70 and high Ku70 expression (Log-rank p=0.0099); with low Ku80 and high Ku80 expression (Log-rank p=0.00087); (**G**). overall survival of patients receiving anti-PDL1 therapy with low Ku70 and high Ku70 expression (Log-rank p=0.043); with low Ku80 and high Ku80 expression (Log-rank p=0.099); (**H**). overall survival of patients receiving Pembrolizumab with low Ku70 and high Ku70 expression (Log-rank p=0.0025); with low Ku80 and high Ku80 expression (Log-rank p=0.00013). (**I**). overall survival of patients receiving anti-CTLA4 therapy with low Ku70 and high Ku70 expression (Log-rank p=0.09); with low Ku80 and high Ku80 expression (Log-rank p=0.077). XRCC5/Ku80, XRCC6/Ku70, ****, p<0.0001; ***, p<0.001.

General Characteristics of the Immune Signatures in HCC

A total of ninety-two immune genes were identified in the immune signatures analyzed in this study. As showed in the volcano plot, enrichment of the immune signatures was analyzed and plotted by Gene Ontology (GO), concerning the biological process (GO-BP), cell component (GO-CC), molecular function (GO-MF). Kyoto Encyclopedia of Genes and Genomes (KEGG), reactive and WikiPathways were used to describe the general characteristics of the immune signatures (Figure 2A–B).

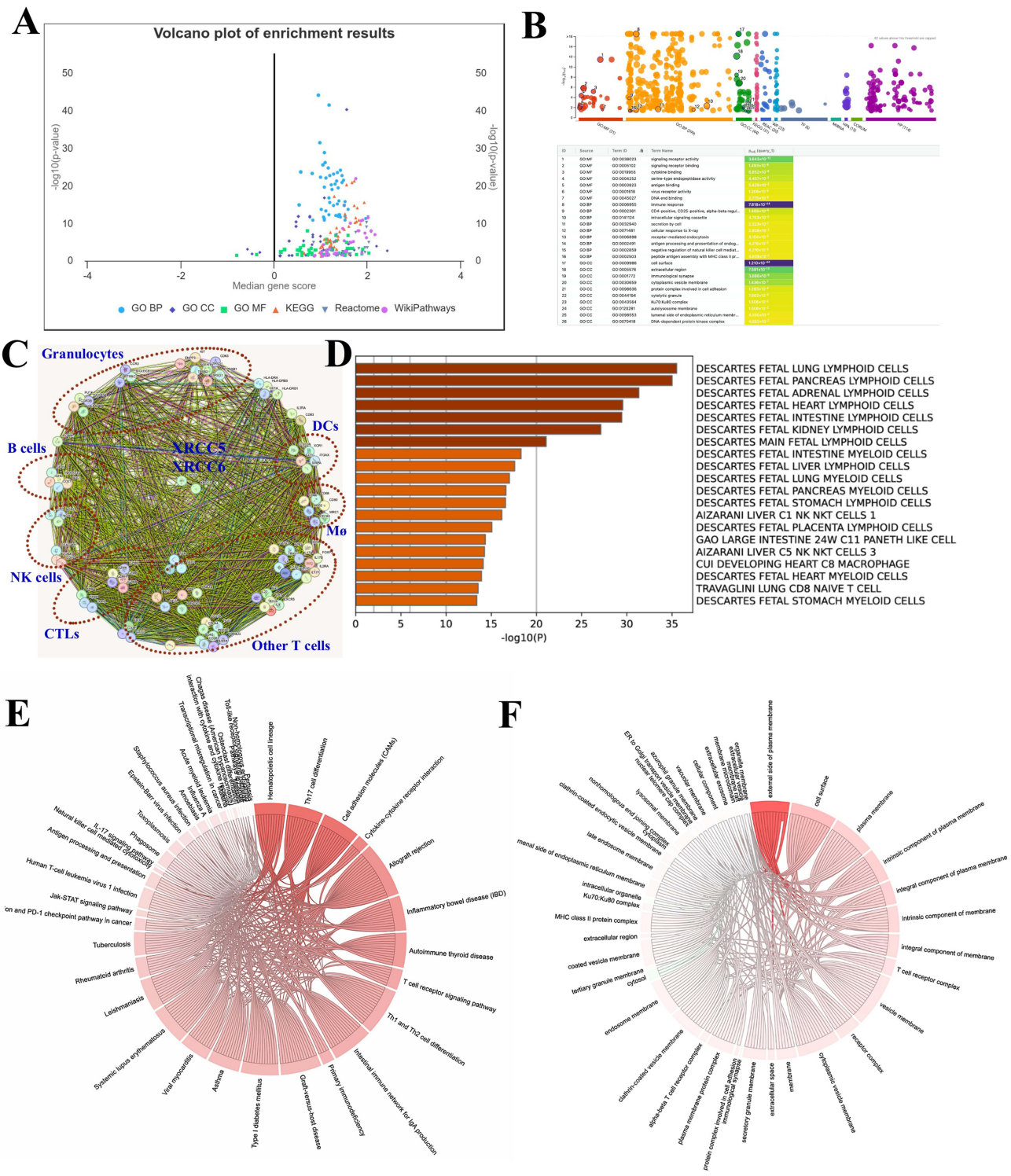

Figure 2 General characteristics of the immune signatures in HCC. (**A**). Volcano plot showed the different enrichment results of all immune signatures used in the study. (**B**). General view of the enrichment results in GO-BP, GO-CC, GO-MF, KEGG, Reactome and WikiPathways. (**C**). PPI showed the various clustered immune cells of myeloid cells and lymphocytes, and their potential connection with Ku70/Ku80. (**D**). GO enrichment showed the cell types of the immune signatures. (**E**). Dependency wheel showed the KEGG enrichment of the immune signatures. (**F**). Dependency wheel showed the GO-CC enrichment of the immune signatures.

In the protein-protein interaction analysis (Figure 2C), both Ku80 (*XRCC5*) and Ku70 (*XRCC6*) were validated in most interactions with these immune genes at protein level, indicating their key roles in immune cell regulation. The immune signatures were further clustered according to immune cell type, including myeloid cells and lymphocytes (Figure 2C–D).

KEGG and GO-CC analyses further indicated that the immune signatures were significantly correlated with a myriad of inflammatory activities and immune-related diseases. This reflects the function of the different immune cell components included in the study (Figure 2E–F).

General Analysis of Ku80, Ku70 and the Immune Signatures in HCC

The expression of Ku80 and Ku70 significantly correlated with HCC immune signature (Figure 3A). The increased expression level of the common antigen for leukocytes, CD45 (protein tyrosine phosphatase receptor type C, PTPRC), indicated better prognosis in HCC patients (HR=0.69, 95% confidence interval [CI] 0.48–0.99, log-rank p=0.042; Figure S1A). This was significantly correlated with the expression of both Ku80 (Pearson correlation r=0.2351, p<0.0001, Figure S1B) and Ku70 (Pearson correlation r=0.1249, p=0.0156, Figure S1C).

Myeloid Cells

Similarly, the myeloid cell marker CD11b (integrin subunit alpha M, ITGAM) significantly correlated with the expression of Ku80 (Figure S1D) and Ku70 (Figure S1E). The correlation chord diagram showed that several clusters of

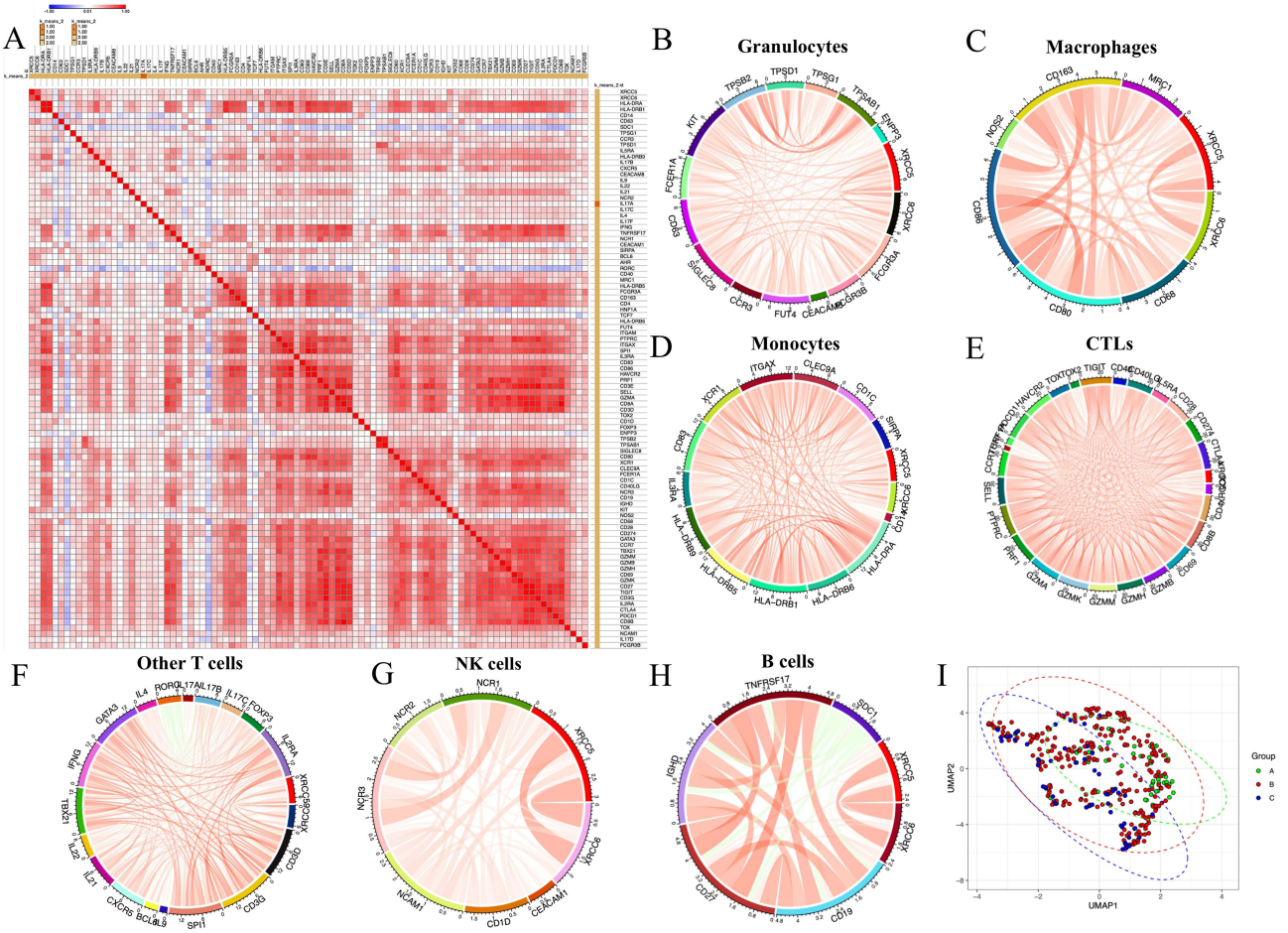

Figure 3 General analysis of Ku80, Ku70 and the immune signatures of HCC.(**A**). Correlation heatmap showed the overall correlation of the expression of Ku80, Ku70 and the immune signatures of HCC. (**B**). Correlation chord diagram showed the correlation between granulocyte signatures with Ku80 and Ku70 expression. (**C**). Correlation chord diagram showed the correlation between macrophages signatures with Ku80 and Ku70 expression. (**D**). Correlation chord diagram showed the correlation between monocyte signatures with Ku80 and Ku70 expression. (**E**). Correlation chord diagram showed the correlation between cytotoxic lymphocytes (CTLs) signatures with Ku80 and Ku70 expression. (**F**). Correlation chord diagram showed the correlation between other T cell signatures with Ku80 and Ku70 expression. (**G**). Correlation chord diagram showed the correlation between NK cell signatures with Ku80 and Ku70 expression. (**H**). Correlation chord diagram showed the correlation between B cell signatures with Ku80 and Ku70 expression. (**I**). UMAP showed the three different patient sub-groups clustered according to the expression of Ku70, Ku80 and immune signatures. Scale bar indicated high correlation (red/max) to low correlation (blue/minimum) in the heatmap.

myeloid cells were significantly correlated with Ku80 and Ku70 in HCC. These included common granulocytes, macrophages, and monocytes (Figure 3B–D).

Among the markers of tumor-associated neutrophils (TANs), only the expression level of CD66b indicated a better prognosis (Figure S2A). CD15 expression was associated with worse prognosis in HCC, although the difference was not statistically significant (Figure S2B). The expression level of Ku80 significantly correlated with CD16A (Fc gamma receptor IIIa, FCGR3A), CD16B (Fc gamma receptor IIIc, FCGR3B) and CD15, while Ku70 was significantly correlated with that of CD16/FCGR3A, CD15 and CD66a (Figure S2C–2H).

For tumor-associated macrophages (TAMs), high CD68 expression indicated worse clinical outcomes in HCC (Figure S3A). CD68 was significantly correlated with Ku70 (Table S1) but not with Ku80 (N.S., Table S1). As for M1-TAMs markers, high expression of ins/NOS2 (nitric oxide synthase, NOS) was indicative of good prognosis (Figure S3B), but was not correlated with either Ku80 or Ku70 expression. However, CD80 significantly correlated with Ku70 (Figure S3C) and Ku80 (Figure S3D). Similarly, CD86 significantly correlated with Ku70 (Figure S3E) and Ku80 (Figure S3F). Therefore, both Ku proteins correlated with $CD80^+$ and $CD86^+$ M1-like macrophages, but not with ins/$NOS2^+$ macrophages.

In M2-TAMs, only high CD206 expression indicated better clinical outcomes in patients with HCC (Figure S3G). CD206 expression did not correlate with those of Ku80 (N.S., Table S1) or Ku70 (N.S., Table S1). The expression of CD163, another M2 marker, significantly correlated with the expression of Ku70 (Figure S3H) and Ku80 (Figure S3I).

Other granulocyte clusters including basophils, eosinophils, mast cells, monocytes and Dendritic cells, are described in Table S1.

Lymphocytes

The correlation chord diagram showed that several clusters of lymphocytes were significantly correlated with Ku80 and Ku70 expression. These included CTLs, NK cells, B cells and other T cells (Figure 3E–H). These results indicate that Ku80 and Ku70 are both vital factors for the regulation of different tumor-associated lymphocyte sub-groups. UMAP was performed and plotted to show that the three different patient sub-groups were clustered according to the expression of Ku70, Ku80 and immune signatures (Figure 3I).

CD3 is the common T cell markers. The following three transcripts were identified, CD3D, CD3E and CD3G. Higher expression of CD3E and CD3G, but not CD3D (Figure S4A), indicated good prognosis (Figure S4). And both Ku proteins significantly correlated with all CD3 subtypes (Figure S4).

CD8, granzymes (GZMs) and Perforin (PRF1) are functional CTL markers. They were all indicators of good clinical prognosis, CD8A (Figure S5A), CD8B (Figure S5B), Perforin/PRF1 (Figure S5C), GZMA (Figure S5D), GZMB (Figure S5E), GZMH (Figure S5F), GZMK (Figure S5G), GZMM (Figure S5H). Both Ku80 and Ku70 significantly correlated with all CTL markers in HCC (Figure 3E, Figure S6–S7, Table S1).

High expression of exhausted T cells markers (PD-1/PDCD1 and CD274/PD-L1) significantly correlated with Ku80 and Ku70 (Table S1). Progenitor exhausted T cells (Tex) markers included TIM-3/HAVCR2, TCF1/HNF1A and TCF7. These also significantly correlated with Ku80 and Ku70 (Table S1). Terminally exhausted T cells (tax) can be clustered according to the markers thymocyte selection associated high mobility group box (TOX), TOX-2 and T cell immunoreceptor with Ig and ITIM domains (TIGIT). Both Ku80 and Ku70 were significantly correlated with tax markers (Table S1).

Combined Analysis of Ku70, Ku80, $CD8^+$ CTL in HCC Tissues and Patient Survival

Although higher expression of Ku70 and Ku80 indicated worse survival outcome in patients with HCC, they could be good predictor for CTL-centered immunotherapies, as shown in solid tumors (Figure 1). We then decided to further understand how the CTL-centered immunotherapies can benefit patients with high Ku70/Ku80 expression. Subsequently, we analyzed Ku70, ku80 and the common CTL marker, CD8 (CD8A and CD8B).

As shown in the results from TCGA database, higher expression of Ku80 and Ku70 was risk factors for HCC patient survival (Figure 1B and D). But higher CD8+ CTL signatures was protective factor for HCC prognosis (Figure S5). In further combined analyses, higher Ku80 expression and lower CD8A expression indicated the worst survival outcomes among all HCC patient subgroups (Figure 4A). In contrast, low Ku80 and high CD8A expression indicated the best

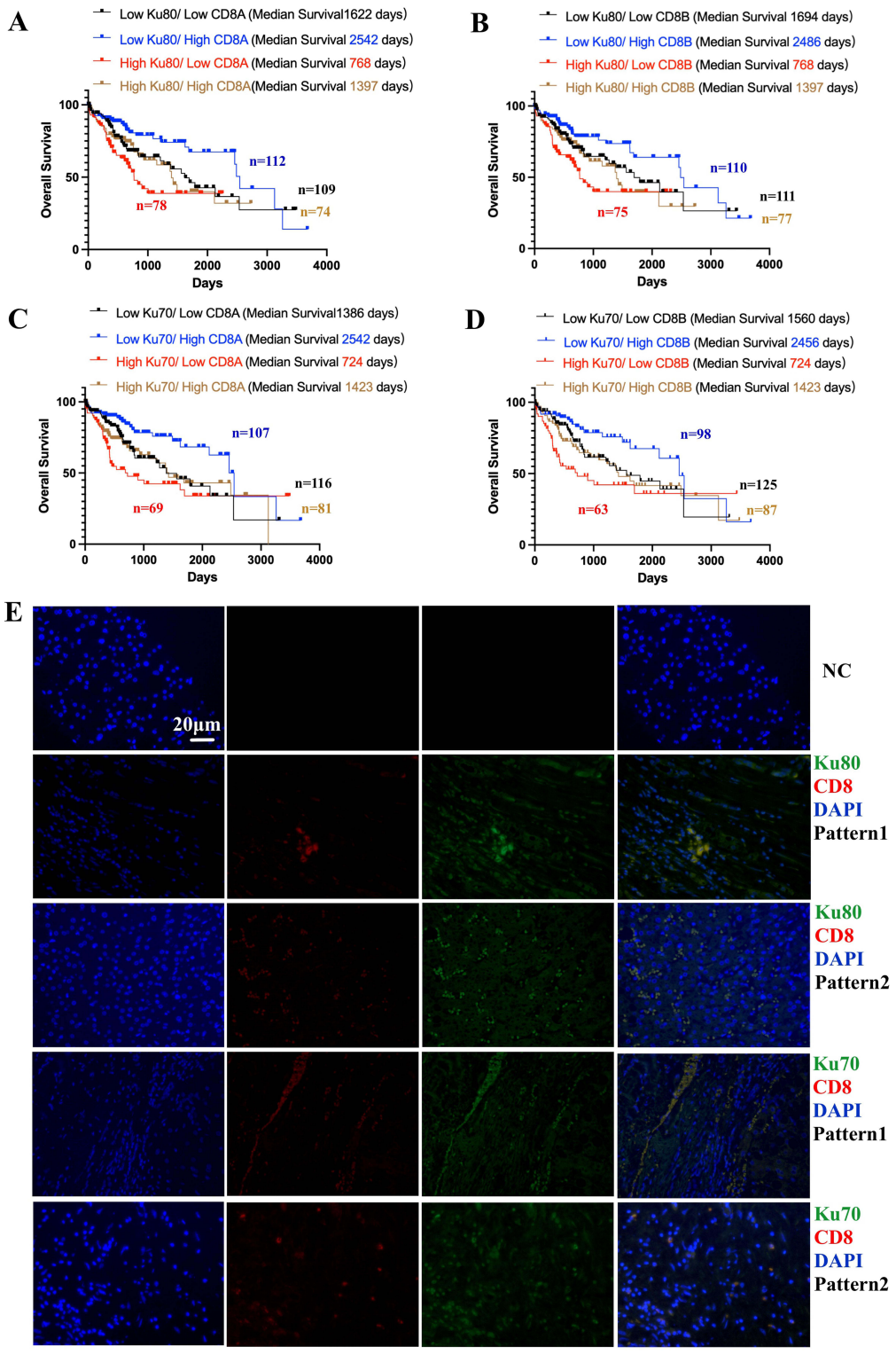

Figure 4 Combined analysis of Ku70, Ku80, CD8+ T cells in TCGA database and their tissue expression pattern validated by co-localized immunofluorescence staining. (**A**). Combined analysis showed the expression of Ku80 and CD8A and the survival outcomes in HCC patients (log-rank p=0.0014). High Ku80/low CD8A vs low Ku80/ high CD8A showed HR=2.64 (95% CI 1.532 to 4.549, log-rank p=0.0003). (**B**). Combined analysis showed the expression of Ku80 and CD8B and the survival outcomes in HCC patients (log-rank p=0.0023). High Ku80/low CD8B vs low Ku80/high CD8B showed HR=2.504 (95% CI 1.462 to 4.289, log-rank p=0.0002). (**C**). Combined analysis showed the expression of Ku70 and CD8A and the survival outcomes in HCC patients (log-rank p=0.0023). High Ku70/low CD8A vs low Ku70/high CD8A showed HR=2.713 (95% CI 1.566 to 4.699, log-rank p<0.0001). (**D**). Combined analysis showed the expression of Ku70 and CD8A and the survival outcomes in HCC patients (log-rank p=0.0019). High Ku70/low CD8B vs low Ku70/high CD8B showed HR=2.763 (95% CI 1.566 to 4.877, log-rank p=0.0001). (**E**). immunofluorescence co-localization showed the different expression patterns Ku70/CD8+ CTL and Ku80/CTL. Ku80/Ku70/CD8+CTLs/DAPI.

survival among all HCC patient subgroups (Figure 4A). High Ku80/low CD8A vs low Ku80/high CD8A showed an HR of 2.64 (Figure 4A).

Likewise, high Ku80 and low CD8B expression indicated the worst survival outcomes in all HCC patients (Figure 4B), whereas low Ku80 and high CD8B expression indicated the best survival (Figure 4B). High Ku80/low CD8B vs low Ku80/high CD8B showed an HR of. 2.504 (Figure 4B).

High Ku70 and low CD8A expression indicated the worst survival outcomes in HCC patients (Figure 4C). In contrast, low Ku70 and high CD8A expression indicated the best survival (Figure 4C). High Ku70/low CD8A vs low Ku70/high CD8A showed an HR of 2.713 (Figure 4C).

High Ku70 and low CD8B expression indicated the worst survival outcomes in HCC patients (Figure 4D), whereas low Ku70 and high CD8B expression indicated the best survival (Figure 4D). High Ku70/low CD8B vs low Ku70/high CD8B showed an HR of 2.763 (Figure 4D).

To further investigate the expression pattern of Ku70, Ku80 and $CD8^+$ CTL in HCC tissues, co-localized immunofluorescence staining was performed (Figure 4E). There were mainly two different expression patterns (scattered and gathered) concerning the relative co-localization of the two Ku proteins and $CD8^+$ CTL in HCC tissues (Figure 4E). Ku70 and Ku80 were mainly expressed in cancer cells, although they were also overexpressed in some of the $CD8^+$ CTL (Figure 4E).

Validating the Clinical Implications of Ku70, Ku80 and $CD8^+$ CTL in HCC Tissues and Patient Survival from Our Center

We then validated the correlation between Ku70, Ku80 and $CD8^+$ CTL and their clinical implications in patients with HCC from our center. General characteristic of the 120 patients with HCC was presented (Table 1). High expression of Ku70, Ku80 and $CD8^+$ CTL was an independent risk factor for post-surgical HCC patients, according to the univariate and multivariate analyses (Table 2).

Table 1 General Characteristics of the 120 hCC Patients in Our Center

Variables		Number of Patients	Percentage of Patients (%)
Age	≥60y <60y	45 75	37.5 62.5
Sex	Female Male	26 94	21.7 78.3
Tumor size	Diameters <5cm Diameters ≥5cm	64 56	53.3 46.7
AFP	>20ng/mL ≤20ng/mL	70 50	58.3 41.7
Multiple tumors (≥2)	Yes No	39 81	32.5 67.5
MVI	Yes No	70 50	58.3 41.7
Pathological stage	I II–IV	54 66	45 55
cirrhosis	Yes No	92 28	76.7 23.3

(*Continued*)

Table 1 (Continued).

Variables		Number of Patients	Percentage of Patients (%)
BCLC stage	A B	100 20	83.3 16.7
Viral hepatitis	Yes No	103 24	85.8 14.2
LN metastasis	Yes No	12 108	10 90
ALT	>80U/L ≤80U/L	43 77	35.8 64.2
Total bilirubin	>1.0mg/dL (17.1μmol/L) ≤1.0mg/dL (17.1μmol/L)	43 77	35.8 64.2
Albumin	<35g/L ≥35g/L	22 98	18.3 81.7
Child-Pugh	A B	120 0	100 0
Post-operative TACE treatment	Yes No	78 42	65 35

Table 2 Univariate and Multivariate Analysis for Overall Survival, the 120 hCC Patients in Our Center

	Univariate analysis	Multivariate analysis			
	Overall Survival	Overall Survival			
	p value	p value	HR	95.0% CI	
				Lower	Upper
Age, ≥60y vs <60y	0.183	NA	NA	NA	NA
Sex, Female vs Male	0.875	NA	NA	NA	NA
Tumor size, DM, <4cm vs ≥4cm	0.89	0.934	1.033	0.482	2.211
AFP, >20ng/mL vs ≤20ng/mL	0.577	0.213	1.628	0.756	3.506
Multiple tumors (≥2), Yes vs No	0.177	0.131	1.878	0.829	4.254
MVI, Yes=1 vs No	<0.001	0.005	3.598	1.474	8.787
Pathological stage, I vs II–IV	0.014	NA	NA	NA	NA
Cirrhosis, Yes vs No	0.23	0.002	5.284	1.826	15.289
BCLC stage, B vs A	<0.001	0.084	2.466	0.887	6.858
Viral hepatitis, No vs Yes	0.789	NA	NA	NA	NA
LN metastasis, Yes vs No	0.219	0.833	1.127	0.372	3.415
ALT, >80U/L vs ≤80U/L	0.208	NA	NA	NA	NA
Total bilirubin, >1.0mg/dL (17.1μmol/L) vs ≤1.0mg/dL (17.1μmol/L)	0.929	NA	NA	NA	NA
Albumin, <35g/L vs ≥35g/L	0.719	NA	NA	NA	NA
Child Pugh, B vs A	NA	NA	NA	NA	NA
TACE, Yes vs No	0.191	0.195	0.626	0.308	1.272
Ku80, high vs low	0.003	0.041	2.325	1.035	5.221
Ku70, high vs low	0.002	0.035	2.328	1.062	5.101
CD8, high vs low	0.023	0.007	0.355	0.168	0.749

Ku80 and Ku70 expression in HCC tissues significantly correlated with the number of $CD8^+$ CTL (Figure 5A–B). Patients with HCC were divided into three groups according to Ku80 and Ku70 expression (Figure 5C–D). The number of $CD8^+$CTL was significantly higher in patients with high Ku80 (Figure 5C) and Ku70 expression (Figure 5D).

We validated the clinical implications of Ku70, Ku80 and $CD8^+$ CTL in HCC. The combined analysis showed that high Ku80 expression and fewer CD8+CTL indicated the worst survival outcomes in HCC patients (Figure 5E). In

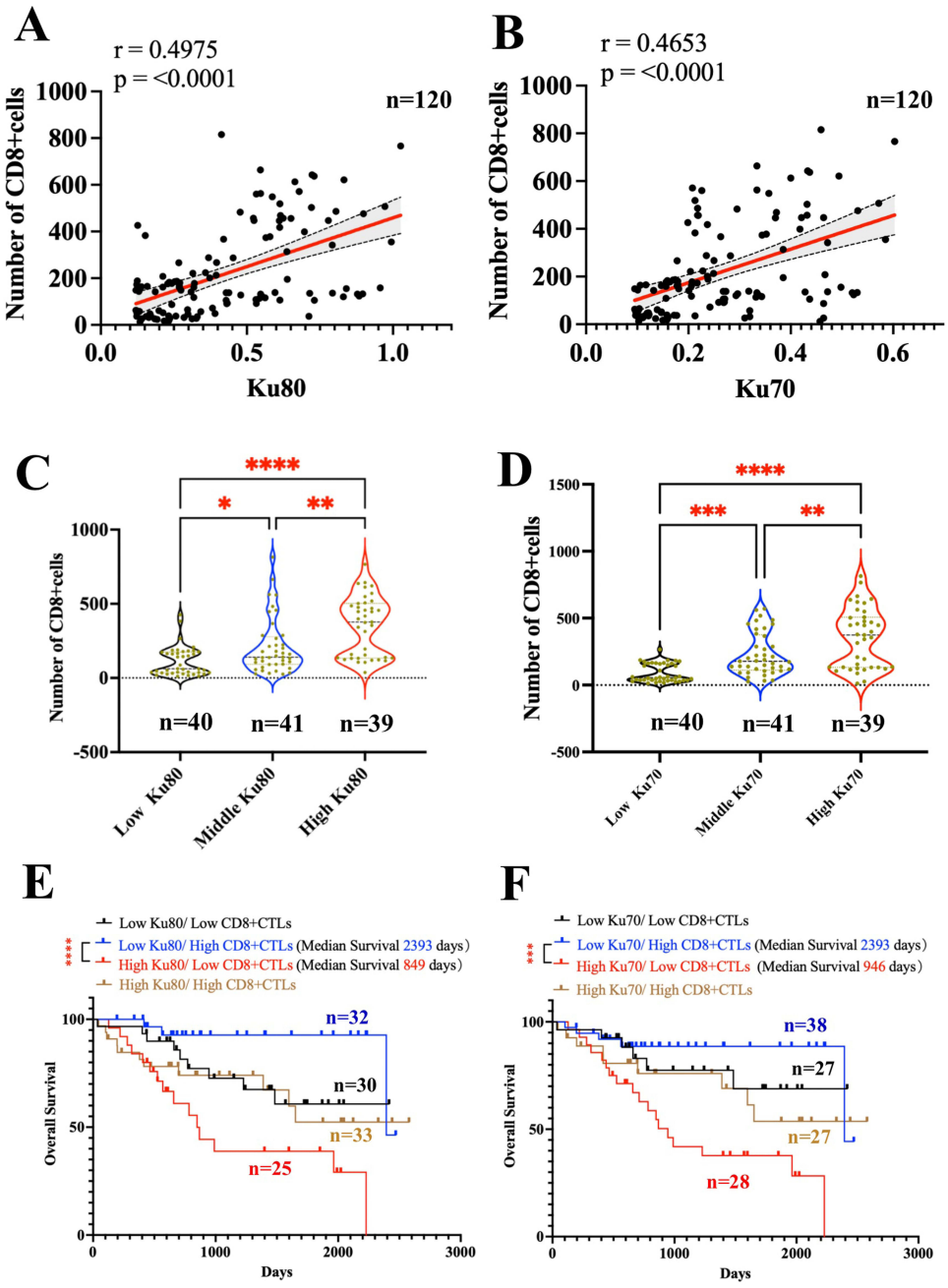

Figure 5 Combined analysis of Ku70, Ku80 and CD8+ T cells in HCC samples from our center. Clinicopathological analysis of 120 patients was performed according to the total expression of Ku70 and Ku80 and the number of CD8+CTL under immunofluorescence staining. (**A**). correlation of the expression of Ku80 and the number of CD8+ CTL (Spearman r=0.4975 p<0.0001, n=120). (**B**). correlation of the expression of Ku70 and the number of CD8+ CTL (Spearman r=0.4653 p<0.0001, n=120). (**C**). the number of CD8+CTL in three groups of HCC patients divided according to the expression of Ku80. (**D**). the number of CD8+CTL in three groups of HCC patients divided according to the expression of Ku70. (**E**). Combined analysis showed the expression of Ku80 and the number of CD8+CTL and the survival outcomes in HCC patients (log-rank p=0.0014, n=120). High Ku80/low CD8+CTLs (n=25) vs low Ku80/high CD8+CTL (n=32) showed HR=8.482 (95% CI 3.259 to 22.07, log-rank p<0.0001). (**F**). Combined analysis showed the expression of Ku70 and the number of CD8+CTL and the survival outcomes in HCC patients (log-rank p=0.001, n=120). High Ku70/low CD8+CTL (n=28) vs low Ku70/high CD8+CTL (n=38) showed HR=5.402 (95% CI 2.346 to 12.44, log-rank p=0.0001). *, p<0.05; **, p<0.01; ***, p<0.001; ****, p<0.0001.

contrast, low Ku80 expression and a higher number of $CD8^+$CTL indicated the best survival (Figure 5E). High Ku70 expression and few $CD8^+$CTL indicated the worst survival outcomes in HCC patients (Figure 5F), while low Ku70 expression and a higher number of $CD8^+$CTL indicated the best survival (Figure 5F).

Discussion

We performed a complete analysis of the roles of Ku80 and Ku70 in the HCC immune microenvironment and their contribution to immunotherapy. In our study, Ku80 and Ku70 expression positively correlated with the enrichment of most immune cell markers. These included myeloid cell markers of neutrophils and eosinophils and lymphocyte markers of $CD8^+$CTL, regulatory T cells and NKCs, etc. Therefore, a high expression of Ku80 and Ku70 indicates a hot immune infiltration signature in HCC. Meanwhile, up-regulation of Ku80 and Ku70 also indicated better anti-PD1 and anti-PDL1 treatments outcomes, but did not correlate with the anti-CTLA4 treatment. Higher Ku70/Ku80 expression combined with a low number of $CD8^+$CTL indicated the worst survival outcomes in patients with HCC. Low Ku70/Ku80 expression combined with a high number of CD8+CTLs indicated the best survival.

The fact that the two Ku proteins are correlated with hotter immune signatures can be attributed to their many regulatory roles in the immune system. Mechanistically, genomic stresses and DNA damage are frequent events that occur during the rapid activation and proliferation of immune cells, which often requires DNA repairing by Ku80, Ku70 and NHEJ components.[28] Both Ku molecules are closely involved in the activation of several immune responses. For example, the DNA-binding ability of Ku proteins can trigger potent cyclic GMP-AMP synthase (cGAS)/stimulator of interferon response camp interactor 1 (STING) inflammatory pathway, which is responsive to DNA-mediated immune reactions.[6,29] In addition, Ku proteins regulate different immune cell types by correcting the enormous DNA disruptions happening during the maturation and functions of these cells,[6] including both myeloid cells and lymphocytes.[30] In contrast, activation of Ku80 and Ku70 triggers immune response via transcriptional up-regulation of various pro-inflammatory factors, such as TNF-α, IL-1β and IL-6.[18,30,31] These pro-inflammatory cytokines are known to recruit and activate the many immune cell elements in cancer and causes subsequent effects on target immune cells.[32–35] Therefore, Ku80 and Ku70 show pervasive pro-inflammatory effects in HCC.

Increased expression K80 and Ku70 expression indicates the clinical responsiveness to several immunotherapies. The effects of immunotherapy depend largely on the active tumor-killing of CTLs. Under physiological conditions, the activation and functions of lymphocytes are well under the regulation of Ku80 and Ku70.[36] We have further confirmed the relationships between Ku70/Ku80 and intra-tumoral lymphocytes, including T cells, B cells and NKCs. In previous studies, lymphocyte diversity is found to be regulated by Ku80/Ku70 at different levels. For example, the activity of Ku70/80 binding to DNA breaks and the level of phosphorylated Ku80 are most evident in naïve T cells.[7] In addition, during the development of immune cells, double strand breaks are commonly repaired by Ku proteins and NHEJ elements, ensuring the generation of diverse immunoglobulins and T cell receptors. Therefore, the Ku 70/80 and NHEJ pathway is an innate part of the variable–diversity–joining/V(D)J recombination and class switch process during lymphocyte maturation.[21,37,38] From this point of view, it is reasonable to suggest that there are innate connections between the high Ku70/Ku80 and enrichment of intra-tumoral lymphocytes. Such connections can partially explain the favorable treatment outcomes of immunotherapies in patients with higher Ku70/Ku80 expression.

However, Ku proteins also play immune-hostile roles in cancer, which can explain why the patients with increased Ku70/Ku80 expression but decreased CTL signatures bear the worst clinical outcomes in our study. For example, Ku80 participates in the process of DNA damage-induced apoptosis during the late phase of T cell activation, closely related to T cell depletion.[39] Furthermore, increased Ku70 expression is a protective factor for tumor cells survival and immune evasion.[40] From another point of view, CTL can directly regulate the Ku proteins in cancer cells. For example, the granzyme A from functional and activated CTL can on the other hand, cleaves and modifies Ku70, causing the caspase-independent cell deaths in the target such as like cancer.[40,41] Under such circumstances, the increase of Ku proteins in HCC can reflect a decreased CTL functions or number, implicating a hostile immune microenvironment. To understand such roles, more studies should be designed concerning the complicated mechanisms of Ku70 and Ku80 in regulating different immune cells within HCC.

To cope with such situations, inhibition of the NHEJ molecules has been developed as a strategy to overcome therapy resistance and to boost intra-tumoral immunity, in cancers where there is a decrease in the number of CTL and increased Ku proteins, such as in the triple negative breast cancer.[9,42] The same strategy can also be adopted for HCC patients with decreased CTL but high Ku80/Ku70 expression to maximize the efficacy of immunotherapy. However, as in the study, Ku70 and Ku80 are closely related to almost all immune elements within the HCC tumor tissues, indicating that simple inhibition or activation of either molecule can bring off-target immune effects. In addition, the inappropriate application of immunotherapy can trigger intrinsic DNA repair promoting tumor survival and poor patient outcomes.[43] Therefore, a careful selection of HCC patients with specific Ku protein and immune signatures may lead to treatment success.

This study has several limitations. Because this study was designed to understand the correlation between Ku80/Ku70 and the immune microenvironment in HCC, in-depth mechanistic studies are lacking. However, our data suggest that Ku protein expression and CTL activation status could be detected in patients with HCC before receiving immunotherapy. Therefore, the detection of Ku proteins should be a part of the clinical decision making, specifically for immunotherapy or chemoimmunotherapy. Although there are strategies targeting Ku proteins and NHEJ, significant clinical success in patient treatment remains elusive. In the results from recent clinical trials, treatments based on tyrosine kinase inhibitors plus immune checkpoint inhibitors have shown an improved anti-tumor effect.[44] It is also noteworthy that the Ku proteins can contribute to the selection of more suitable patients for the combined therapies, but more research is still needed. In future studies, the combination of Ku protein-targeted therapy and immunotherapy should also be considered as combined therapy to regulate the tumor immune microenvironment.

Conclusion

In sum, high Ku80 and Ku70 expression indicates a "hotter" immune infiltration signature in HCC. Patients with increased expression of Ku80 and Ku70 and $CD8^+$CTL signatures benefit the most from CTL-centered immunotherapies. However, novel therapies are needed to target Ku80/Ku70 and boost the CTL signatures in patient sub-groups with high Ku70/Ku80 expression but low CTL signatures.

Data Sharing Statement

All data not included in the manuscript is available from the supplementary materials.

Consent for Publication

All authors have read and approved the manuscript.

Ethics Statement

All protocols for experiments concerning human samples, including analysis of data from publicly available data, were reviewed and approved by the Research Ethics Committee of the Fifth Affiliated Hospital of Sun Yat-sen University (reference number 2019-L-120-1). Due to its retrospective nature, the study did not contain recorded information about patients' privacy. Therefore, patients' informed consent could be exempted, but all patients signed an informed consent form when admitted in hospital. Patient data confidentiality was strictly maintained. The study was conducted in compliance with the Declaration of Helsinki.

Acknowledgments

The authors would like to acknowledge and thank the TCGA database, from the National Cancer Institute GDC data portal, and the many scientists who get involved and put their efforts to make it an even better database for oncological research.

Author Contributions

All authors made a significant contribution to the work reported, whether that is in the conception, study design, execution, acquisition of data, analysis and interpretation, or in all these areas; took part in drafting, revising or critically reviewing the article; gave final approval of the version to be published; have agreed on the journal to which the article has been submitted; and agree to be accountable for all aspects of the work.

Funding

This work was funded by the National Natural Science Foundation of China (grant number 82272105), Guangdong Basic and Applied Basic Research Foundation (grant number 2020A1515010203, 2022A1515011244, 2022A1515012382, 2023A1515011521, 2023A1515010475), Medical Scientific Research Foundation of Guangdong Province of China (A2017421, 2016116212141586).

Disclosure

All authors declare no conflicts of interests.

References

1. Casadei-Gardini A, Rimini M, Tada T, et al. Atezolizumab plus bevacizumab versus lenvatinib for unresectable hepatocellular carcinoma: a large real-life worldwide population. *Eur J Cancer*. 2022;180:9–20. doi:10.1016/j.ejca.2022.11.017
2. D'Alessio A, Fulgenzi CAM, Nishida N, et al. Preliminary evidence of safety and tolerability of atezolizumab plus bevacizumab in patients with hepatocellular carcinoma and Child-Pugh A and B cirrhosis: a real-world study. *Hepatology*. 2022;76(4):1000–1012. doi:10.1002/hep.32468
3. Wu J, Liu W, Qiu X, et al. A noninvasive approach to evaluate tumor immune microenvironment and predict outcomes in hepatocellular carcinoma. *Phenomics*. 2023;3(6):549–564. doi:10.1007/s43657-023-00136-8
4. Yang KD, Zhang X, Shao MC, et al. Aconite aqueous extract inhibits the growth of hepatocellular carcinoma through CCL2-dependent enhancement of natural killer cell infiltration. *J Integr Med*. 2023;21(6):575–583. doi:10.1016/j.joim.2023.10.002
5. Cheu JW, Wong CC. The immune microenvironment of steatotic hepatocellular carcinoma: current findings and future prospects. *Hepatol Commun*. 2024;8(9). doi:10.1097/HC9.0000000000000516
6. Morchikh M, Cribier A, Raffel R, et al. HEXIM1 and NEAT1 long non-coding RNA form a multi-subunit complex that regulates DNA-mediated innate immune response. *Mol Cell*. 2017;67(3):387–399.e385. doi:10.1016/j.molcel.2017.06.020
7. Scarpaci S, Frasca D, Barattini P, et al. DNA damage recognition and repair capacities in human naïve and memory T cells from peripheral blood of young and elderly subjects. *Mech Ageing Dev*. 2003;124(4):517–524. doi:10.1016/S0047-6374(03)00030-7
8. Bao K, Ma Y, Li Y, et al. A di-acetyl-decorated chromatin signature couples liquid condensation to suppress DNA end synapsis. *Mol Cell*. 2024;84(7):1206–1223.e1215. doi:10.1016/j.molcel.2024.02.002
9. Ma C, Qin Y, Wang Y, et al. Targeting DNA-PKcs promotes anti-tumoral immunity via triggering cytosolic DNA sensing and inducing an inflamed tumor immuno-microenvironment in metastatic triple-negative breast cancer. *Genes Dis*. 2023;10(5):1809–1811. doi:10.1016/j.gendis.2023.01.001
10. Shu Y, Jin X, Ji M, et al. Ku70 binding to YAP alters PARP1 ubiquitination to regulate genome stability and tumorigenesis. *Cancer Res*. 2024;84(17):2836–2855. doi:10.1158/0008-5472.CAN-23-4034
11. Tang M, Chen G, Tu B, et al. SMYD2 inhibition-mediated hypomethylation of Ku70 contributes to impaired nonhomologous end joining repair and antitumor immunity. *Sci Adv*. 2023;9(24):eade6624. doi:10.1126/sciadv.ade6624
12. Pfister D, Núñez NG, Pinyol R, et al. NASH limits anti-tumour surveillance in immunotherapy-treated HCC. *Nature*. 2021;592(7854):450–456. doi:10.1038/s41586-021-03362-0
13. Kruse B, Buzzai AC, Shridhar N, et al. CD4(+) T cell-induced inflammatory cell death controls immune-evasive tumours. *Nature*. 2023;618(7967):1033–1040. doi:10.1038/s41586-023-06199-x
14. Maalej KM, Merhi M, Inchakalody VP, et al. CAR-cell therapy in the era of solid tumor treatment: current challenges and emerging therapeutic advances. *Mol Cancer*. 2023;22(1):20. doi:10.1186/s12943-023-01723-z
15. Granito A, Muratori L, Lalanne C, et al. Hepatocellular carcinoma in viral and autoimmune liver diseases: role of CD4+ CD25+ Foxp3+ regulatory T cells in the immune microenvironment. *World J Gastroenterol*. 2021;27(22):2994–3009. doi:10.3748/wjg.v27.i22.2994
16. Sallmyr A, Henriksson G, Fukushima S, et al. Ku protein in human T and B lymphocytes: full length functional form and signs of degradation. *Biochim Biophys Acta*. 2001;1538(2–3):305–312. doi:10.1016/S0167-4889(01)00081-7
17. Muller C, Dusseau C, Calsou P, et al. Human normal peripheral blood B-lymphocytes are deficient in DNA-dependent protein kinase activity due to the expression of a variant form of the Ku86 protein. *Oncogene*. 1998;16(12):1553–1560. doi:10.1038/sj.onc.1201676
18. Sun H, Li Q, Yin G, et al. Ku70 and Ku80 participate in LPS-induced pro-inflammatory cytokines production in human macrophages and monocytes. *Aging*. 2020;12(20):20432–20444. doi:10.18632/aging.103845
19. Yu X, Li Y, Yang P, et al. BCL11B promotes T-cell acute lymphoblastic leukaemia cell survival via the XRCC5/C11ORF21 axis. *Clin Transl Med*. 2024;14(2):e1580. doi:10.1002/ctm2.1580
20. Liang Z, Kumar V, Le Bouteiller M, et al. Ku70 suppresses alternative end joining in G1-arrested progenitor B cells. *Proc Natl Acad Sci U S A*. 2021;118:21.
21. Zan H, Tat C, Qiu Z, et al. Rad52 competes with Ku70/Ku86 for binding to S-region DSB ends to modulate antibody class-switch DNA recombination. *Nat Commun*. 2017;8(1):14244. doi:10.1038/ncomms14244
22. Zou B, Liu X, Gong Y, et al. A novel 12-marker panel of cancer-associated fibroblasts involved in progression of hepatocellular carcinoma. *Cancer Manage Res*. 2018;10:5303–5311. doi:10.2147/CMAR.S176152
23. Kolberg L, Raudvere U, Kuzmin I, et al. g:Profiler—interoperable web service for functional enrichment analysis and gene identifier mapping (2023 update). *Nucleic Acids Res*. 2023;51(W1):W207–W212. doi:10.1093/nar/gkad347
24. Backes C, Keller A, Kuentzer J, et al. GeneTrail—advanced gene set enrichment analysis. *Nucleic Acids Res*. 2007;35(suppl_2):W186–W192. doi:10.1093/nar/gkm323
25. Zhou Y, Zhou B, Pache L, et al. Metascape provides a biologist-oriented resource for the analysis of systems-level datasets. *Nat Commun*. 2019;10(1):1523. doi:10.1038/s41467-019-09234-6
26. Zhao J, Lin E, Bai Z, et al. Cancer-associated fibroblasts induce sorafenib resistance of hepatocellular carcinoma cells through CXCL12/FOLR1. *BMC Cancer*. 2023;23(1):1198. doi:10.1186/s12885-023-11613-8

27. Wang B, Tang C, Lin E, et al. NIR-II fluorescence-guided liver cancer surgery by a small molecular HDAC6 targeting probe. *EBioMedicine*. 2023;98:104880. doi:10.1016/j.ebiom.2023.104880
28. Cerutti A, Schaffer A, Goodwin RG, et al. Engagement of CD153 (CD30 ligand) by CD30+ T cells inhibits class switch DNA recombination and antibody production in human IgD+ IgM+ B cells. *J Immunol*. 2000;165(2):786–794. doi:10.4049/jimmunol.165.2.786
29. Sakai C, Ueda K, Goda K, et al. A possible role for proinflammatory activation via cGAS-STING pathway in atherosclerosis induced by accumulation of DNA double-strand breaks. *Sci Rep*. 2023;13(1):16470. doi:10.1038/s41598-023-43848-7
30. Shi L, Qiu D, Zhao G, et al. Dynamic binding of Ku80, Ku70 and NF90 to the IL-2 promoter in vivo in activated T-cells. *Nucleic Acids Res*. 2007;35(7):2302–2310. doi:10.1093/nar/gkm117
31. Ghonim MA, Ju J, Pyakurel K, et al. Unconventional activation of PRKDC by TNF-α: deciphering its crucial role in Th1-mediated inflammation beyond DNA repair as part of the DNA-PK complex. *J Inflamm*. 2024;21(1):14. doi:10.1186/s12950-024-00386-x
32. King HAD, Pokkali S, Kim D, et al. Immune activation profiles elicited by distinct, repeated TLR agonist infusions in rhesus macaques. *J Immunol*. 2023;211(11):1643–1655. doi:10.4049/jimmunol.2300424
33. Di Meglio A, Havas J, Pagliuca M, et al. A bio-behavioral model of systemic inflammation at breast cancer diagnosis and fatigue of clinical importance two years later. *Ann Oncol*. 2024;35(11):1048–1060. doi:10.1016/j.annonc.2024.07.728
34. Etzion O, Bareket-Samish A, Yardeni D, et al. Namodenoson at the crossroad of metabolic dysfunction-associated steatohepatitis and hepatocellular carcinoma. *Biomedicines*. 2024;12(4):848. doi:10.3390/biomedicines12040848
35. Ishtiaq SM, Arshad MI, Khan JA. PPARγ signaling in hepatocarcinogenesis: mechanistic insights for cellular reprogramming and therapeutic implications. *Pharmacol Ther*. 2022;240:108298. doi:10.1016/j.pharmthera.2022.108298
36. Jiang W, Estes VM, Wang XS, et al. Phosphorylation at S2053 in Murine (S2056 in Human) DNA-PKcs Is dispensable for lymphocyte development and class switch recombination. *J Immunol*. 2019;203(1):178–187. doi:10.4049/jimmunol.1801657
37. Fell VL, Schild-Poulter C. The Ku heterodimer: function in DNA repair and beyond. *Mutat Res Rev Mutat Res*. 2015;763:15–29. doi:10.1016/j.mrrev.2014.06.002
38. Malu S, Malshetty V, Francis D, et al. Role of non-homologous end joining in V(D)J recombination. *Immunol Res*. 2012;54(1–3):233–246. doi:10.1007/s12026-012-8329-z
39. Wang Y, Sun H, Wang J, et al. DNA-PK-mediated phosphorylation of EZH2 regulates the DNA damage-induced apoptosis to maintain T-cell genomic integrity. *Cell Death Dis*. 2016;7(7):e2316. doi:10.1038/cddis.2016.198
40. Zhu P, Zhang D, Chowdhury D, et al. Granzyme A, which causes single-stranded DNA damage, targets the double-strand break repair protein Ku70. *EMBO Rep*. 2006;7(4):431–437. doi:10.1038/sj.embor.7400622
41. Lieberman J. Granzyme A activates another way to die. *Immunol Rev*. 2010;235(1):93–104. doi:10.1111/j.0105-2896.2010.00902.x
42. Gout J, Perkhofer L, Morawe M, et al. Synergistic targeting and resistance to PARP inhibition in DNA damage repair-deficient pancreatic cancer. *Gut*. 2021;70(4):743–760. doi:10.1136/gutjnl-2019-319970
43. Kornepati AVR, Boyd JT, Murray CE, et al. Tumor intrinsic PD-L1 promotes DNA repair in distinct cancers and suppresses PARP inhibitor-induced synthetic lethality. *Cancer Res*. 2022;82(11):2156–2170. doi:10.1158/0008-5472.CAN-21-2076
44. Stefanini B, Ielasi L, Chen R, et al. TKIs in combination with immunotherapy for hepatocellular carcinoma. *Expert Rev Anticancer Ther*. 2023;23(3):279–291. doi:10.1080/14737140.2023.2181162